

SUPPLEMENTARY INFORMATION

P2X receptor channels show three-fold symmetry in ionic charge selectivity and unitary conductance

Liam E. Browne, Lishuang Cao, Helen E. Broomhead, Laricia Bragg, William Wilkinson & R. Alan North

Supplementary Methods

Molecular and cell biology A concatemer was constructed that contained four restriction sites (*NheI*, *SacII*, *NotI* and *ApaI*) that do not appear normally in the cDNA of other rat subunits (P2X1 - P2X5). Met¹ residues were removed in the second and third subunits, and the encoding of restriction sites and frame spacers introduced a minimal linker region between subunits: the linker was -GRG- between the first and second subunits, and -GRR- between the second and third. Each subunit also included a C-terminal EE-epitope tag (EYMPME). The final product was ligated into pcDNA3.1(+) vector (Invitrogen, Paisley, UK).

The P2X2 wild type concatenated trimer was constructed in three steps. The P2X2 cDNAs were amplified by PCR using PfuTurbo (Stratagene, Agilent Technologies, Berkshire UK) and primers containing the unique restriction sites. The first PCR product contained a 5' *NheI* site and 3' *SacII* and *ApaI* sites: it was cut at *NheI* and *ApaI*, and then ligated into a vector to produce the intermediate product Construct A. The second product contained a 5' *SacII* and 3' *NotI* and *ApaI*. The *SacII* and *ApaI* sites of both PCR product and Construct A were cut, and ligated with the vector to produce Construct B. The third PCR product contained 5' *NotI* and 3' *ApaI* sites, and both the PCR product and Construct B were cut and ligated into the vector to form the final P2X2 concatemer. Between each step, the intermediate constructs were transformed into chemically competent bacteria, overnight cultures grown, and mini-preparations of plasmid DNA were collected and digested with *NheI* and *ApaI* to ensure that an insert of the correct size was present. To introduce mutations into the concatemer, the subunits were cut from the concatemer at the according restriction sites and ligated into a shuttle vector. Site-directed mutagenesis was performed on the monomer P2X2 subunit using the Stratagene QuikChange method. The resulting mutation was then PCR amplified with appropriate 5' and 3' restriction sites on the PCR primer, and the product was ligated back into the concatemer to produce the final product. To confirm the final constructs each subunit was removed and sequenced as a PCR product and sub-cloned into the shuttle vector pPCR-Script Amp SK(+) (Stratagene) where the entire coding

region was confirmed. Expression detection was measured with both anti-P2X2 and anti-EYMPME antibodies (Bethyl Laboratories, Montgomery, TX).

The wild type and mutant P2X2 subunits (0.1 – 1 μ g), or the concatenated cDNAs (1 μ g), were transiently co-expressed together with GFP (0.1 μ g) vector in HEK293 cells (by Lipofectamine 2000; Invitrogen, San Diego, CA). Transfected cells were seeded on glass coverslips coated with poly-L-lysine.

Western blot and surface expression Cell surface protein was labeled using EZ-link sulfo-NHS-LC-biotin (Pierce, Cramlington, UK). Confluent cells (one 25 cm³ culture flask per sample) were washed three times in PBS, pH 8.0, and incubated in 1 ml of PBS containing 0.5 mg/ml biotin for 30 min at 4°C. After washing, cells were centrifuged, and pellets lysed in PBS containing 2% Triton X-100 and antiproteases (complete EDTA; Roche, Lewes, UK) for 1 h at 4°C. After centrifugation (16,000 X g; 2 min) to remove debris, total protein samples were removed and assayed for protein content using a protein assay kit (Bio-Rad, Hemel Hempstead, UK). Biotinylated surface protein in the cell lysate was bound to immuno-pure immobilized streptavidin beads (Pierce) overnight at 4°C. After washing in PBS containing 0.2% Triton X-100, SDS-PAGE sample buffer was added and the samples were boiled (5 min; 100°C) to release cell surface protein. Samples were separated on 10% Nu-PAGE gels (Invitrogen) and transferred to nitrocellulose membranes. Western blotting was performed according to standard protocols and proteins were visualized using rabbit anti-EYMPME primary antibody (Bethyl) and HRP-conjugated secondary antibody (both at 1:5000 dilution), followed by detection using the ECL-plus kit (Amersham Biosciences, Buckinghamshire, UK) and Kodak BioMax light film. Band densities were quantified using GeneSnap/GeneTools software (Syngene, Frederick, MD), and densities were compared using analysis of variance.

Electrophysiological recordings Recordings were made at room temperature 24–72 h after transfection, using outside-out and whole-cell configurations of the patch-clamp technique. Recording pipets were pulled from borosilicate glass (World Precision Instruments, Stevenage, UK) and had resistances of 10–20 M Ω for single channel recording and 2–4 M Ω for whole-cell recording. The usual holding potential was –60 mV for whole-cell and –120 mV for single channel recording. The intracellular (pipette) solution comprised (mM): 147 NaF (or NaCl for the chloride permeability experiments), 10 HEPES, and 10 EGTA. The standard extracellular solution contained (mM): 147 NaCl, 2 KCl, 1 CaCl₂, 1 MgCl₂, 10 HEPES, and 13 glucose. In the permeability experiments, we substituted Cl with gluconate for measurement of P_{Cl}/P_{Na} . All solutions were maintained at pH 7.3 and 300–315 mOsm/l. Chemicals were purchased from Sigma (Poole, UK). Currents were recorded with a

Axopatch 200B amplifier using pClamp 9 software (Molecular Devices, Palo Alto, CA), or an EPC10 amplifier using Patchmaster software (HEKA, Lambrecht Germany). The data were low-pass filtered at 3 kHz with an eight-pole Bessel filter (LHBF-48X; NPI, Tamm, Germany) and digitized at 10 kHz (single channel) or 2 kHz (whole cell). We generated dose–response curves for ATP and other compounds by applying these drugs through an RSC200 rapid perfusion system (Biologic, Claix, France). Agonists were applied for 2 s or, in the case of lower concentrations, until a steady-state current was recorded. For the rectification experiments, series resistance was electronically compensated by 50 – 80% to minimize voltage errors. Current–voltage relationships were obtained from the currents measured during linear voltage ramps (–150 mV to +150 mV in 200 ms) applied at 1 Hz. For chloride permeability measurements, the reversal potential was obtained from the currents measured during voltage ramps (–40 to +40 mV in 200 ms) applied at 1 Hz. The bath and indifferent electrode were connected by an agar bridge containing 3M KCl.

Data analysis Electrophysiological data were analyzed using Clampfit 9 software (Molecular Devices) and QUB program (www.qub.buffalo.edu). Rectification is reported as the ratio of the current observed at +150 or –150 mV to the value computed from linear extrapolation of the I/V relation between +10 and –10 mV. For a linear I/V relation these values would be unity: wild type P2X2 channels show modest inward rectification for inward currents (ratio about 2) and strong inward rectification for outward currents (ratio about 0.2). Relative permeability to chloride ($\alpha = P_{Cl}/P_{Na}$) was calculated by the best fit to the relation between reversal potential of the ATP-evoked current (E_{rev} , mV) and the extracellular chloride concentration ($[Cl]_o$) given by $E_{rev} = 25.2 \ln\{([Na]_o + \alpha [Cl]_i)/([Na]_i + \alpha [Cl]_o)\}$ where $[Na]_o = 151$, $[Na]_i = 172$, and $[Cl]_i = 147$ mM ($1000 \times RT/F = 25.2$ mV). In these experiments, we included other extracellular cations (2 mM K^+ , 1 mM Mg^{2+} , 1 mM Ca^{2+}) in the total for $[Na]_o$, so that strictly α should denote P_{Cl}/P_{cation} . Obvious overlapping of single channel openings were removed manually before the amplitudes were measured by all-points amplitude histograms fit to two or more Gaussian distributions. Pooled data are given as the mean \pm s.e.m. Tests for statistical significance were performed using nonparametric ANOVA.

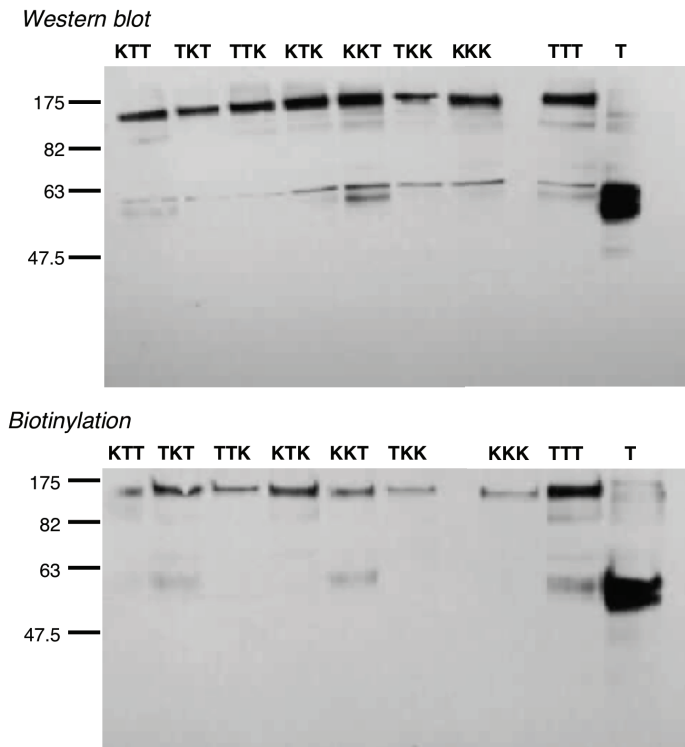
Model building Molecular models were constructed using open-source software [Chimera: Pettersen, E.F., *et al. J. Comput. Chem.* **25**, 1605-1612 (2004); Coot: Emsley, P. & Cowtan, K. *Acta Crystallogr. D Biol. Crystallogr.* **60**, 2126-2132 (2004); MolProbity: Chen, V.B., *et al. Acta Crystallogr. D Biol. Crystallogr.* **66**, 12-21; HOLE: Smart, O.S., Neduvelil, J.G., Wang, X., Wallace, B.A. & Sansom, M.S. *J. Mol. Graph.* **14**, 354-360, 376 (1996).]

Supplementary Table 1

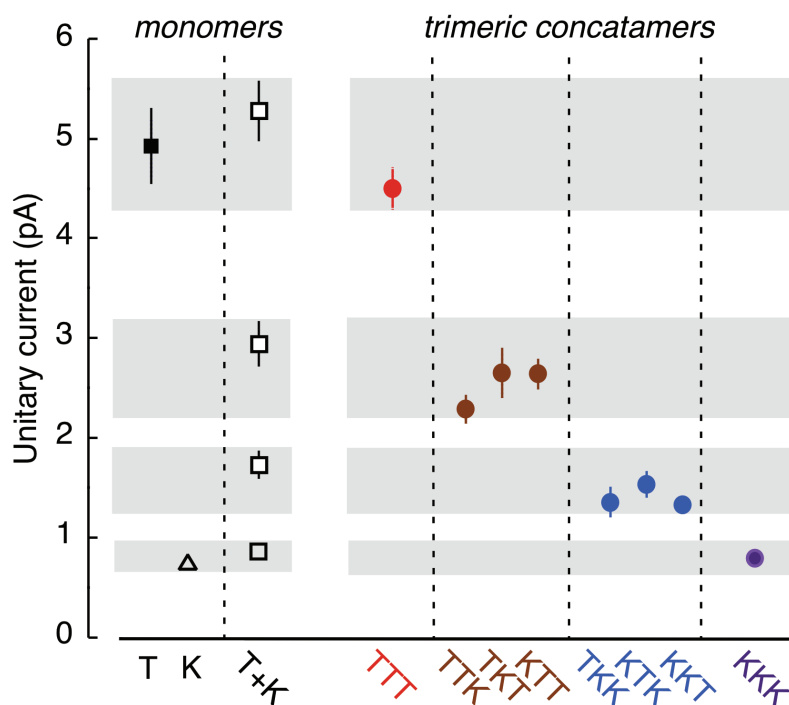
	inward (at -150 mV)		outward (at 150 mV)		P_{Cl}/P_{Na}	
	mean	s.e.m. (n)	mean	s.e.m. (n)	mean	s.e.m. (n)
<i>Monomers</i>						
wild type	1.8	0.1(6)	0.3	0.03(6)	0	0(10)
T339K	2.2	0.3(7)	2.3	0.3(7)	1.8	0.1(12)
T339R	3.0	0.4(5)	3.2	0.6(5)	2.2	0.1(6)
<i>Concatemers</i>						
TTT	1.9	0.2(5)	0.1	0.1(5)	0	0(12)
KTT	1.6	0.1(5)	0.5	0.1(5)	0.21	0.04(9)
TKT	1.8	0.3(7)	0.5	0.2(7)	0.11	0.05(6)
TTK	1.6	0.5(4)	0.5	0.1(4)	0.27	0.06(5)
KKT	2.3	0.2(10)	0.7	0.1(10)	0.12	0.03(9)
KTK	2.2	0.2(9)	1.8	0.1(9)	0.74	0.05(7)
TKK	2.3	0.3(4)	1.2	0.1(4)	0.61	0.06(4)
KKK	1.8	0.3(5)	2.1	0.3(5)	1.3	0.08(4)

Table 1. Rectification index and relative chloride permeability for monomeric and concatenated P2X2 subunits

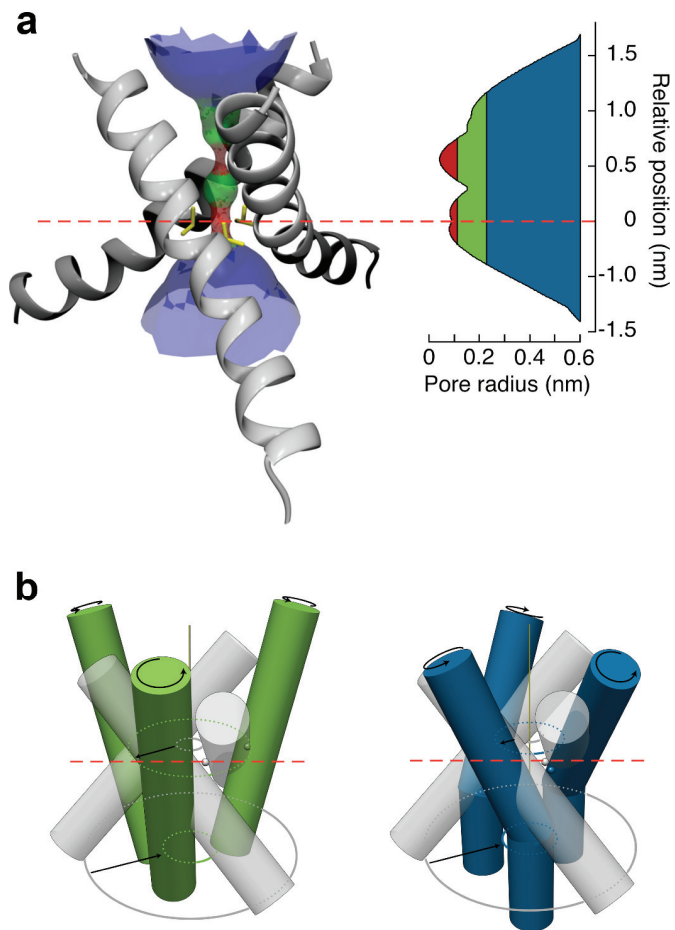
Supplementary Figures



Supplementary Fig. 1. Trimeric protein expression. Western blotting and biotinylation indicated that the predominant form of membrane protein expressed by HEK cells had a molecular weight corresponding to that of a trimer. The exception to this was the trimer KKT, in which a significant amount of monomeric form was also observed at the membrane. Top panel depicts total protein expressed in HEK293 cells (see **Supplementary Methods**). Loading was 10 ng protein per sample, with exposure of 10 s. Bottom panel shows surface protein (see **Supplementary Methods**). Loading was approximately 500 ng protein per sample, with exposure of 60 s. Band sizes for monomer and trimeric P2X2 receptors, seen in both panels, correspond to expected sizes of 60 kDa and 180 kDa, respectively. Protein markers 6 – 175 kDa (New England Biolabs Inc, MA, USA).



Supplementary Fig. 2 Summary of unitary current amplitudes. Left side, summary currents for wild type receptors (T) and T339K receptors (K), and from the mixture (T+K). Right side, currents from concatenated cDNAs of wild-type and mutant P2X2 receptors. Mean currents were estimated from all points histograms fitted with multiple Gaussians: error bars indicate s.e. of mean for 3 – 7 observations. Holding potential -120 mV.



Supplementary Fig. 3 Model of P2X2 receptor pore. (a) Closed pore structure. *Left*, the three TM2 helices of a P2X2 model viewed from the side. Model of the rat P2X2 receptor TM domains generated with Modeller 9v7 using the zebrafish P2X4.1 crystal structure (PDB accession 3H9V) as a template (structure assessed using Coot and MolProbity, and pore surface lining calculated using HOLE; see **Supplementary Methods**). Pore radius represented by color (*red*: $< 1.15 \text{ \AA}$; *green*: $1.15 - 2.3 \text{ \AA}$; and *blue*: $> 2.3 \text{ \AA}$) suggests that there are two constrictions in the pore of the closed P2X2 receptor. One is at T336, and one situated a helical turn lower at T339 (side chains shown in *yellow*). The image was constructed in Chimera and rendered in Blender (see **Supplementary Methods**). *Right*, the same data from HOLE shown in graphical form. Broken red line illustrates level of T339 C α atoms. (b) Possible pore-opening mechanisms. *Left*, simple steepening, rotation and separation of the helices. *Right*, steepening, rotation and separation of outer helices combined with bending at G342. Grey cylinders indicate closed channel. Green (*left*) or blue (*right*) cylinders indicate open channel. Ball (and broken red line) indicates position of T339 C α atoms.